An Empirical Method for Computing Leeside Centerline Heating on the Space Shuttle Orbiter

Vernon T. Helms III*
NASA Langley Research Center, Hampton, Virginia

An empirical method is presented for computing top centerline heating on the Space Shuttle Orbiter at simulated re-entry conditions. It is shown that the Shuttle's top centerline can be thought of as being under the influence of a swept cylinder flowfield. The effective geometry of the flowfield, as well as top centerline heating, is directly related to oil flow patterns on the upper surface of the fuselage. This relationship allowed the development of an empirical heating method which is derived from turbulent swept cylinder theory. The method takes into account the effects of the vortex-dominated leeside flowfield without actually having to compute the detailed properties of such a complex flow. The heating method closely predicts experimental heat-transfer values on the top centerline of a Shuttle model at Mach 6 and 10 over a wide range in Reynolds number and angle of attack.

Nomenclature

C_L = centerline
C_1, C_2 = experimentally determined coefficients defined in Eq. (4)
$f(\Lambda)$ = arbitrary function of sweep angle defined in Eq. (4)
L = length of wind-tunnel model
M = Mach number
q_c = convective heating rate, local value unless otherwise specified
r = cylinder radius and radius of Shuttle model's upper fuselage
Re = Reynolds number
x = axial length measured from nose of model
α = angle of attack
β = bow shock angle measured with respect to freestream direction
δ = flow deflection angle across bow shock measured with respect to freestream direction
ϵ = surface flow angle and local angle of attack with respect to model's top centerline
η = turbulent swept cylinder correlation parameter
Λ = sweep angle
Λ_{max} = sweep angle at which empirical method predicts zero heating, Eq. (6)
ν = Prandtl-Meyer turning angle

Subscripts

D = cylinder diameter
L = quantity based on model length
l = quantity based on leeside properties
o = freestream stagnation value on a scaled 1-ft radius sphere
s = stagnation value on a sphere of radius r
Λ = quantity at a given sweep angle
∞ = freestream

Presented as Paper 81-1043 at the AIAA 16th Thermophysics Conference, Palo Alto, Calif., June 23-25, 1981; submitted Aug. 24, 1981; revision received July 21, 1982. This paper is declared a work of the U.S. Government and therefore is in the public domain.

*Aerospace Engineer, Aerothermodynamics Branch, Space Systems Division.

Introduction

THE complex nature of leeside flowfield phenomena has long been of interest to many investigators. The advent of the Space Shuttle produced a heightened sense of urgency to develop a basic understanding of leeside flow interactions and their attendant thermodynamic environment. During the Shuttle's development phase, several regions on its leeward side were identified as areas of relatively high heating that could potentially affect thermal protection system design criteria. The top of the fuselage, the top centerline in particular, was one of those areas. This region is dominated by vortices which cause flow impingement and heating. There is currently no computer code that can provide a complete solution for a flowfield of this type, so wind-tunnel tests have been the only means of obtaining quantitative heating data on the Shuttle's leeward centerline. Nevertheless, a variety of relatively simple heating methods have been applied in an attempt to duplicate the experimental results. But the best that can be achieved using this approach is only to bracket the wind-tunnel data.

This paper presents a new empirical method based on swept cylinder theory which closely fits both the magnitude and trend of experimental heating distributions along the leeward centerline of a Space Shuttle model at simulated re-entry conditions. Heat-transfer and oil flow data obtained in wind tunnels at the Langley Research Center were used in the development of this technique. It was found that the heating distribution along the top centerline can be directly related to changes observed in surface flow patterns. These patterns resemble those that would be expected on a cylinder with a different swept angle at each point along its length. An existing theory that was originally designed to correlate turbulent data on the windward centerline of a swept cylinder was modified to satisfy the requirements of the leeside environment. The new method has the advantage over other heating techniques in that it accounts for the influence of the vortex-dominated flowfield above the Shuttle's fuselage without having to actually compute in detail the properties for that kind of flow.

Experimental Data

The unpublished wind tunnel test results used to develop the new technique were obtained in air with the Mach 6 and Mach 10 facilities[1-3] at the Langley Research Center as part of a data base that will be used in analyzing Shuttle re-entry flight data.

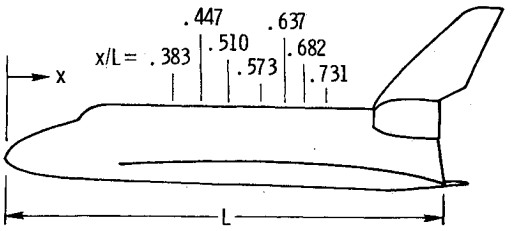

Fig. 1 Thermocouple locations on leeward centerline of Shuttle model.

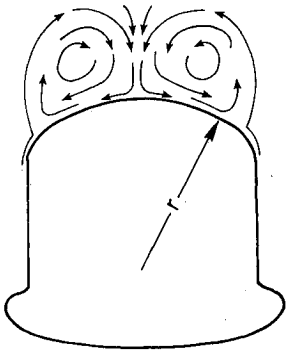

Fig. 2 Typical cross section of Shuttle's fuselage with leeside vortex flow.

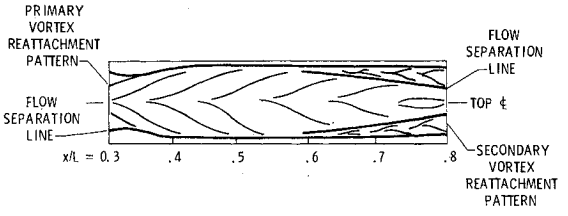

Fig. 3 Oil flow patterns on upper fuselage for $M_\infty = 10$, $\alpha = 20$ deg, $Re_{\infty,L} = 2.4 \times 10^6$.

Leeside heat-transfer measurements were made using a 0.01-scale Shuttle thermocouple model. Thermocouples on the top centerline were located at axial stations $x/L = 0.383$-0.731, as shown in Fig. 1. The model was set at angles of attack of 20-40 deg at 5-deg increments. Length Reynolds numbers based on freestream properties for the Mach 6 tests were 2.7×10^6, 5.4×10^6, and 7.3×10^6. For Mach 10, the test Reynolds numbers were 0.5×10^6, 1.0×10^6, and 2.4×10^6. Oil flow tests, also on a 0.01 scale model, were performed at both Mach numbers using the same freestream conditions and angle-of-attack range as for the heat-transfer measurements. A complete set of oil flow data is available for all test conditions at Mach 10. The surface flow patterns for the Mach 6 test matrix are not as comprehensive, but the data currently in hand represent the entire envelope of angle of attack and Reynolds numbers used in the heat-transfer tests.

Swept Cylinder Analogy

Figure 2 illustrates one aspect of why the Shuttle's leeward centerline can be thought of as having a swept cylinder flowfield. This diagram shows a typical cross section of the Shuttle's fuselage along with a representation of vortex flow patterns above the surface. The top of the fuselage is rounded and is approximated by a segment of a cylinder with radius r. Flow from the counter-rotating vortices begins to merge near the symmetry plane. After being forced downward onto the vehicle's top centerline, the flow spreads outward across the surface. These flow patterns in the vicinity of the top centerline and surface of the fuselage are approximately like those for a cylinder of radius r in a uniform stream with the same properties as the combined flows of the two vortices.

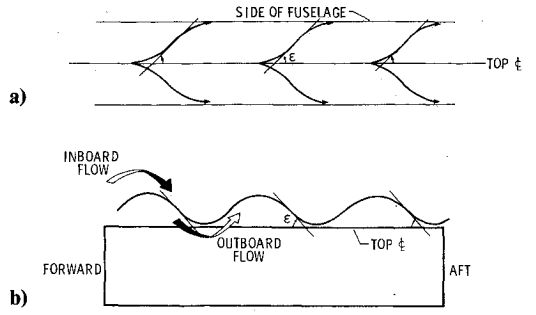

Fig. 4 Simplified view of vortex flow above fuselage: a) Top view; b) Side view.

Definition of a sweep angle is the other aspect of the problem required to complete the analogy with a swept cylinder flowfield. It will now be shown how this information can be derived from measurements of oil flow patterns. Figure 3 shows an example of an oil flow reattachment pattern on top of the 0.01 scale Shuttle model's fuselage. This case is for $M_\infty = 10$, $\alpha = 20$ deg, and $Re_{\infty,L} = 2.4 \times 10^6$. It basically consists of a primary reattachment pattern with a pair of secondary vortices appearing further downstream at these test conditions. The secondary patterns do not enter directly into the empirical formulation. Surface flow directions illustrated in the primary reattachment pattern are similar to what would be expected of flow around a cylinder with a different swept angle at each point along its length. As the surface flow moves outboard from the centerline, it also moves downstream on the model, forming elongated S-shaped patterns. This gives the oil flow a direction outward and away from the centerline at an angle, measured through the inflection point in the pattern, which can be related to the local angle of attack of downward flow from the vortices striking the top of the fuselage. For illustrative purposes, consider the simple case shown in Fig. 4a where the outward angle ϵ is constant at all axial stations. The vortex on either side of the symmetry plane might then be loosely visualized as a circular rotating spiral structure above the fuselage. This structure would appear to have the same sinusoidal waveform as viewed from both the top and the side, as represented in Fig. 4b. Viewed from the top, the apparent inflection point on the outward moving bottom portion for the spiral would correspond to inflection points in the oil flow streaks of the primary reattachment pattern seen in Fig. 3. The angle made between the centerline and a line drawn tangent through this surface inflection point would be equal to the angle between the top of the fuselage and a line drawn tangent to the apparent inflection point as seen from the side. Thus, at least for this idealized case, the outward angle of an oil flow path with respect to the top centerline is equal to the local centerline angle of attack of the flow in the vortices. Under actual circumstances, however, the vortices above the fuselage are not circular. They can be distorted by the presence of the vortex on the opposite side of the symmetry plane and by the top of the fuselage. Also, as shown in Fig. 3, the oil flow angles are not constant, but are a function of axial location.

Since there is no exact way to relate the local angle of attack at a given axial location with the measured angle using the oil flow inflection point directly outboard of that station, it is assumed for simplicity that the two angles are equal. Any difference there may be in these values is accounted for by two experimentally determined constants in the empirical heating equation, which will be discussed shortly. If the measured oil flow angle ϵ is taken to be the local angle of attack on the top centerline, then the sweep angle used in the swept cylinder theory can be expressed in the conventional form

$$\Lambda = 90 \text{ deg} - \epsilon \qquad (1)$$

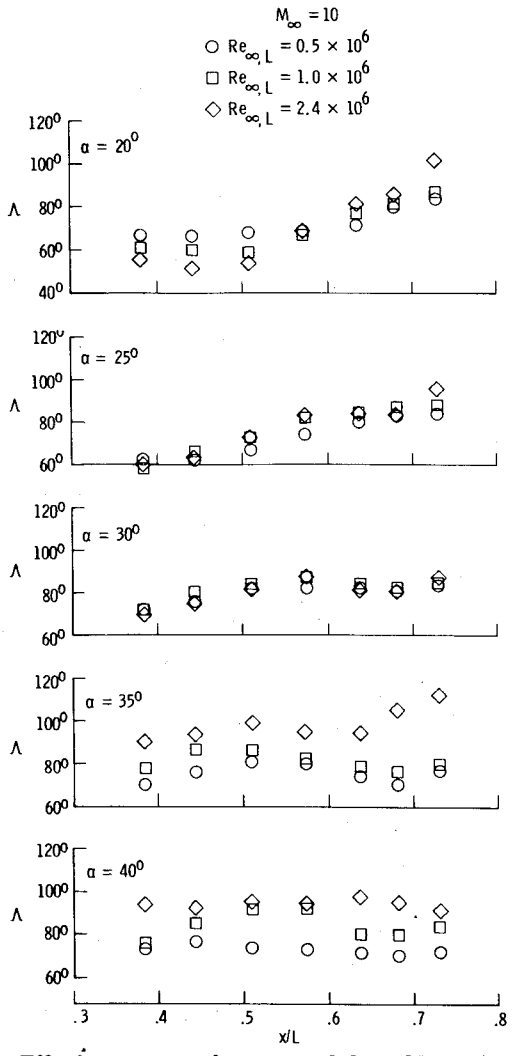

Fig. 5 Effective sweep angles measured from Mach 10 oil flow patterns.

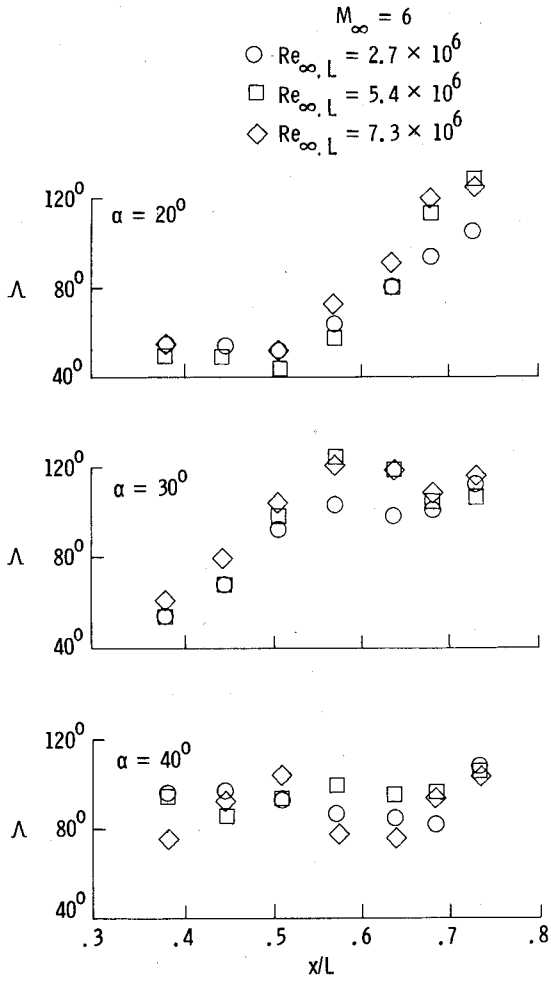

Fig. 6 Effective sweep angles measured from Mach 6 oil flow patterns.

Sweep Angle Measurement and Relation to Heating Distribution

Figures 5 and 6 show the sweep angle Λ plotted as a function of axial location for all angles of attack and Reynolds numbers used in the Mach 10 and Mach 6 oil flow tests. The greatest variation in sweep angle for the Mach 10 data in Fig. 5 occurs at low angle of attack and high Reynolds numbers. At high angle of attack, sweep angles are nearly constant for a given Reynolds number, with higher Reynolds numbers producing larger values of Λ. Trends of the Mach 6 data in Fig. 6 are somewhat the same as for Mach 10, but these sweep angles vary in magnitude over a considerably wider range than the Mach 10 measurements. This indicates a much more dynamic surface flow at the Mach 6 test conditions.

Many of the sweep angles in Figs. 5 and 6 are greater than 90 deg, placing them beyond the range of Λ normally encountered in swept cylinder theory. These large values of Λ are the result of a sign convention that was adopted, which gives a positive sign to ϵ for streamwise flow traveling outboard from the top centerline and a negative sign to inboard flow near the centerline. Inboard flow traveling aft comes about because at some combinations of freestream conditions and angle of attack, the vortices impact the top of the fuselage off the symmetry plane. A portion of the flow then turns inboard, coalescing on the leeward centerline. Or, as in the case shown in Fig. 3, the flow is turned inboard near the trailing end of the primary reattachment pattern by the secondary vortices. In addition, the oil flow angle is defined as being negative in areas of reversed flow. This refers to both inboard and outboard flow traveling forward on the fuselage. These conditions were generally observed at low angles of attack and high Reynolds numbers over the rear portion of the fuselage at Mach numbers of both 6 and 10, with the effect being more extensive at Mach 6. It was necessary to designate both of these reversed flow directions as negative in order to preserve an inverse relation found to exist between Λ and the top centerline heating measurements, which will be discussed below. For this same reason, flow which was occasionally found to cross the top centerline traveling from one side of the model's symmetry plane to the other was also considered to have a negative value of ϵ. Figure 7 illustrates all of these different classes of oil flow angles using diagrams of flow patterns obtained at several different test conditions. In any of these cases where ϵ is negative, the sweep angle defined in Eq. (1) will take on values greater than 90 deg. It therefore seems more appropriate to refer to Λ as an "effective" sweep angle of the purpose of this theory.

The inverse relation between effective sweep angle and top centerline heating mentioned in the preceding paragraph is illustrated in Fig. 8, where the effective sweep angle Λ is paired with the corresponding heating ratio at two different test conditions. Figure 8a is for $M_\infty = 10$, $\alpha = 20$ deg, $Re_{\infty,L} = 2.4 \times 10^6$, and the set of data points for Fig. 8b was taken at $M_\infty = 6$, $\alpha = 30$ deg and $Re_{\infty,L} = 5.4 \times 10^6$. The ratio q_c/q_{c_o} represents the measured local heating rate normalized by the stagnation value on a scaled 1-ft radius sphere in the freestream using the Fay and Riddell[4] method. Both the heating ratio and the effective sweep angle are plotted vs axial location. Clearly, as Λ increases, the level of heating

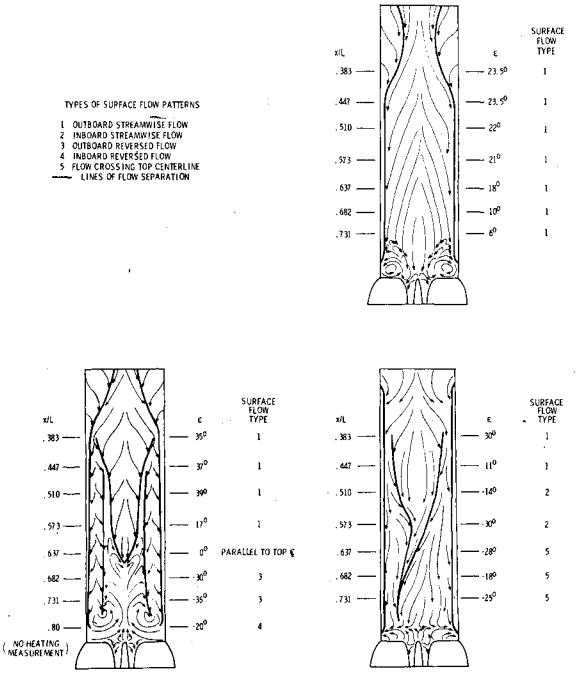

Fig. 7 Leeside oil flow patterns on upper surface of fuselage at three different test conditions: a) $\alpha = 20$ deg, $Re_{\infty,L} = 0.5 \times 10^6$, $M_\infty = 10$; b) $\alpha = 20$ deg, $Re_{\infty,L} = 7.3 \times 10^6$, $M_\infty = 6$; c) $\alpha = 20$ deg, $Re_{\infty,L} = 7.3 \times 10^6$, $M_\infty = 6$.

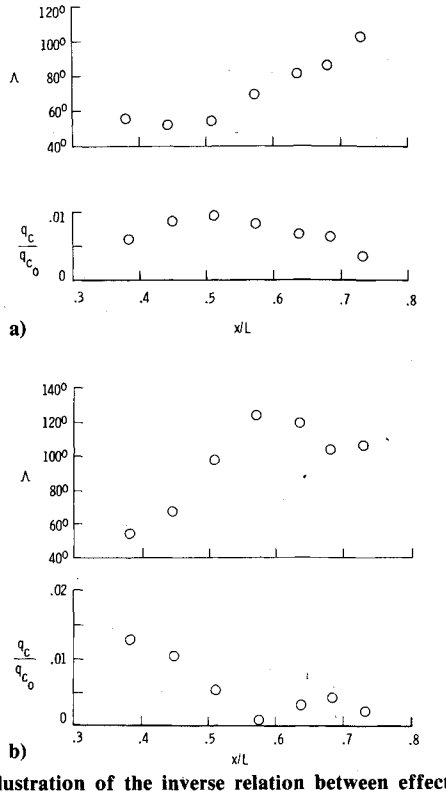

Fig. 8 Illustration of the inverse relation between effective sweep angle and leeward centerline heating rate: $M_\infty = 10$, $\alpha = 20$ deg, $Re_{\infty,L} = 2.4 \times 10^6$; b) $M_\infty = 6$, $\alpha = 30$ deg, $Re_{\infty,L} = 5.4 \times 10^6$.

decreases. Conversely, a decrease in effective sweep angle is accompanied by a rise in the heating rate. Also note that even as effective sweep angle passes 90 deg, the level of heating is still a considerable fraction of the peak value for each of these cases. This inverse relationship was originally noted on those portions of the top centerline influenced by the primary vortex reattachment pattern where sweep angle is less than 90 deg. For this condition, the classical definition of sweep angle is directly related to Λ as defined here. However, heating rates decline smoothly in making the transition from top centerline locations where ϵ is positive and Λ is less than 90 deg to locations in the domain of other surface flow patterns where Λ is greater than 90 deg. Permitting Λ in this theory to become greater than 90 deg is simply a mathematical convenience which allows the inverse sweep angle-heating rate relationship to be extended without interruption to top centerline locations associated with extremely complex surface flow patterns. Reciprocal relationships between effective sweep angle and heating rate similar to those in Fig. 8 were found at all other test conditions as well.

Empirical Heating Equation and Flowfield Assumptions

The question of laminar vs turbulent flow on the upper surface of the Space Shuttle's fuselage is unresolved. However, Zakkay et al.[5] and Bertin et al.[6] have shown that heating rates over a large portion of the leeside centerline on Shuttle configurations seem to be closely related to a turbulent boundary-layer solution for quite a wide range of conditions at Mach 6 and Mach 10. This result focused attention in the present study on turbulent swept cylinder heating techniques, but all existing swept cylinder methods were designed to predict heating on the windward surface. Boundary-layer development on the windward centerline of a swept cylinder, with a uniform freestream and constant sweep angle, should be quite different from that on the Shuttle's leeward centerline where sweep angle and local flow properties are constantly changing. It could therefore be expected that existing turbulent heating equations must be modified in order to satisfy the requirements of the Shuttle's leeside environment. The following discussion describes the steps involved in modifying a turbulent swept cylinder technique developed by W.A. Johnson[7] and its successful application to the measured leeward centerline heating rates on the 0.01 scale Shuttle model.

The swept cylinder theory derived by Johnson made use of turbulent data[8-11] taken across the supersonic speed range for Reynolds numbers from approximately 0.1×10^6 to 4×10^6 and sweep angles up to 75 deg. These measurements were organized into a ratio of turbulent centerline heating at a given sweep angle to the laminar stagnation line heating rate for $\Lambda = 0$ deg. This heating ratio exhibited large variations as a function of Reynolds number. Since turbulent and laminar heating are proportional to $Re^{-0.2}$ and $Re^{-0.5}$, respectively, then the ratio of turbulent centerline to laminar stagnation heating should be proportional to $Re^{0.3}$. Incorporating this relationship into the heating ratio made it possible to remove the Reynolds number dependency of the data using the parameter

$$\eta = \frac{q_{c_\Lambda}}{Re_{\infty,D}^{0.3} q_{c_{\Lambda=0\,\text{deg}}}} \tag{2}$$

with Reynolds number based on freestream conditions and cylinder diameter. After curve fitting the correlated data points, Johnson's turbulent swept cylinder equation for the windward centerline was presented as

$$q_c = 0.75 q_{c_s} Re_{\infty,D}^{0.3} \{0.01714 + 0.01235 \sin[3.53(\Lambda - 10\,\text{deg})]\} \tag{3}$$

where q_c is the local convective heating rate and q_{c_s} is the stagnation value for a sphere in the freestream with a radius equal to that of the cylinder. The coefficients and the trigonometric function in brackets represent the best curve fit to the available data. This last set of terms is equivalent to the parameter η and it modifies the stagnation line value of

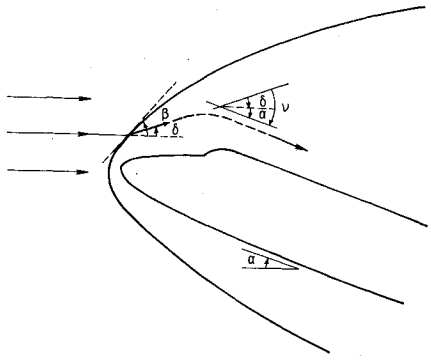

Fig. 9 Flowfield model used to compute leeside properties.

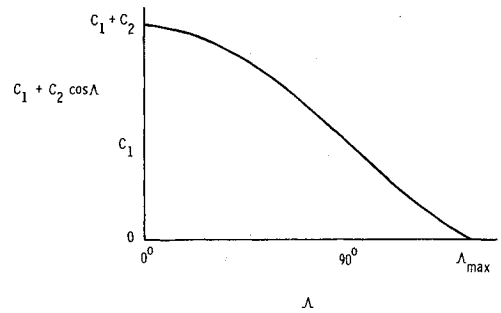

Fig. 10 Dependence of heating rate on effective sweep angle.

heating to account for the fact that the cylinder is at some sweep angle Λ with respect to the oncoming flow. This method is one of several heat-transfer options in the MINIVER[12] aerodynamic heating computer program. MINIVER was used to provide flow properties and associated theoretical heating levels to be discussed in the remainder of this paper.

Equation (3) was derived for sweep angles up to 75 deg. It has already been shown that effective sweep angles measured from oil flow patterns far exceed this value. There is also the concern raised earlier about differences in boundary-layer development on windward and leeward centerlines. These considerations indicate the need for different coefficients and a different function of sweep angle in the bracketed portion of Eq. (3) in order to accommodate the Shuttle's leeside environment. Therefore, the empirical heating equation takes on the basic form

$$q_c = 0.75 q_{c_s} Re_{l,D}^{0.3} [C_1 + C_2 f(\Lambda)] \tag{4}$$

where C_1 and C_2 are constants that must be solved for using experimental data and $f(\Lambda)$ is presumed to be a trigonometric function of effective sweep angle. The radius of the 0.01 scale Shuttle model's upper fuselage is the geometric length used to compute Reynolds number and stagnation point heating in Eq. (4). As before, q_{c_s} is evaluated using the Fay-Riddell method. Both Reynolds number and reference stagnation heating are calculated using local properties in the leeside flowfield. The assumptions made in computing those flow properties will first be explored and then a solution to the function $f(\Lambda)$ will be discussed.

An integral part of the empirical method being formulated here is the procedure established to compute leeside local flow properties used in the heat-transfer calculations. Figure 9 illustrates the simple flowfield model that was employed. This diagram reduces the path that freestream flow must take to reach the upper surface of the fuselage to its most basic form. For a given angle of attack α, freestream flow is processed through a bow shock of angle β. The flow is deflected through an angle δ which is a function of β and freestream Mach number. A real-gas Prandtl-Meyer expansion is then applied and the flow is turned through an angle ν, which is the sum of α and δ, that brings it parallel to the top centerline. This is a convenient stopping point in the expansion because no attempt is made to simulate downward flow angles of the vortices near the symmetry plane which display an intricate dependence on Mach number, Reynolds number, angle of attack, and axial location. Also, bringing the flow parallel to the top centerline represents a flow direction with respect to the vehicle's upper surface which can be repeated regardless of angle of attack or surface flow conditions. Local flow properties resulting from the expansion are used to compute Reynolds number and stagnation line heating in Eq. (4). These quantities are constant for a given set of freestream conditions and angle of attack. Once they are determined, the heating distribution along the top centerline is strictly a function of sweep angle.

A more realistic view of flow processes affecting top centerline heating would have to include impingement on the canopy as well as flow from all along the side of the fuselage which separates and becomes entwined in the leeside vortices. Conditions in these segments of the flowfield will depend on geometric parameters such as shape, size, and location of the canopy, fuselage cross-sectional design, and the position of the wind-body junction. The individual effects on the leeside thermodynamic environment of these sources are unknown, but their collective influence is present in the experimental heat-transfer data. Since the constants C_1 and C_2 must be determined using the experimental data, the contributions of such complex flow interactions as well as the general vortex flowfield above the fuselage will automatically be accounted for in the empirical heating equation.

The function $\cos\Lambda$ satisfies the inverse relationship between heating rate and effective sweep angle illustrated in Fig. 8. Substituting this term for $f(\Lambda)$ in Eq. (4) yields

$$q_c = 0.75 q_{c_s} Re_{l,D}^{0.3} (C_1 + C_2 \cos\Lambda) \tag{5}$$

The dependence of heating rate in Eq. (5) on effective sweep angle is demonstrated in Fig. 10 where the quantity $C_1 + C_2\cos\Lambda$ is plotted as a function of Λ. This figure shows that maximum heating occurs at $\Lambda = 0$ deg. This is in keeping with the assumption of a turbulent boundary layer on the Shuttle's leeward centerline, although experimental studies on the windward centerline of swept cylinders have indicated the presence of a laminar boundary layer at very small sweep angles. The term $C_2\cos\Lambda$ decreases toward zero as Λ increases to 90 deg, and q_c has a finite value at $\Lambda = 90$ deg. For $\Lambda > 90$ deg, $C_2\cos\Lambda$ becomes negative and q_c continues to decrease with increasing Λ until $q_c = 0$ at

$$\Lambda_{max} = 180 \text{ deg} - \cos^{-1}(C_1/C_2) \tag{6}$$

Equation (6) represents the maximum value of Λ for which the empirical heating method can be used.

The only unknown independent variable in the procedure outlined above is the bow shock angle β. There is no direct way of calculating where freestream flow must cross the bow shock in order to have an effect on leeward centerline heating. Therefore, the value of β to be used in this theory was determined by an iterative method using data for $M_\infty = 10$ and $Re_{\infty,L} = 2.4 \times 10^6$, mainly at $\alpha = 20$ deg, but also including a limited number of data points at other angles of attack. Different values for C_1 and C_2 were used with a range of shock angles in Eq. (5) until a combination was found that produced nearly the correct level of heating. This also established the validity of the $\cos\Lambda$ term in correctly representing the trend of heating distribution along the upper centerline. The approximate set of values for the two coefficients resulting from this procedure gave good results when used with a shock angle β equal to twice the angle of attack. The values of C_1 and C_2 were then refined by solving Eq. (5)

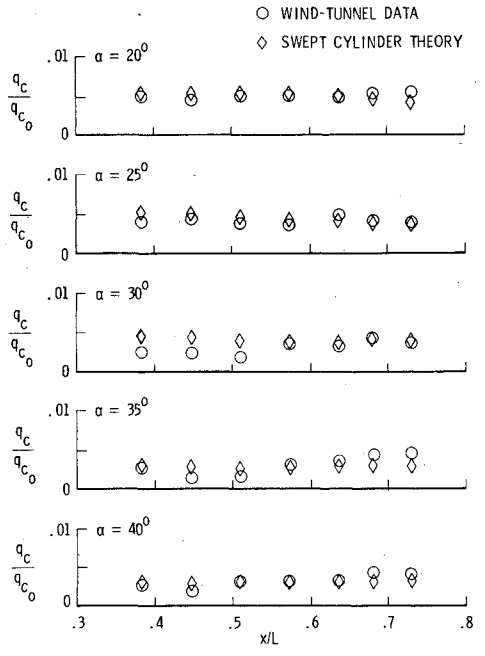

Fig. 11 Comparison of empirical swept cylinder theory with wind tunnel measurements for $M_\infty = 10$ and $Re_{\infty,L} = 0.5 \times 10^6$.

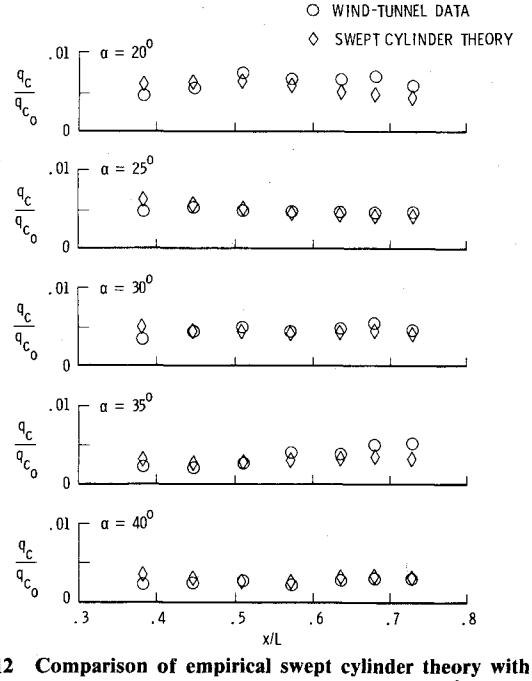

Fig. 12 Comparison of empirical swept cylinder theory with wind tunnel measurements for $M_\infty = 10$ and $Re_{\infty,L} = 1.0 \times 10^6$.

simultaneously for pairs of data points at $\alpha = 20$ deg, each point having a different heating rate and effect sweep angle. The resulting sets of numbers were averaged giving C_1 and C_2 the values

$$C_1 = 0.002975 \quad \text{and} \quad C_2 = 0.003428$$

Substituting these numbers into Eq. (6) yields a maximum sweep angle of 150.2 deg, the angle at which the empirical method will predict zero heating. This should allow a great diversity of flow patterns to be treated. The empirical swept cylinder heat-transfer equation for the Shuttle's leeward centerline now becomes

$$q_c = 0.75 q_{c_s} Re_{l,D}^{0.3} (0.002975 + 0.003428 \cos\Lambda) \qquad (7)$$

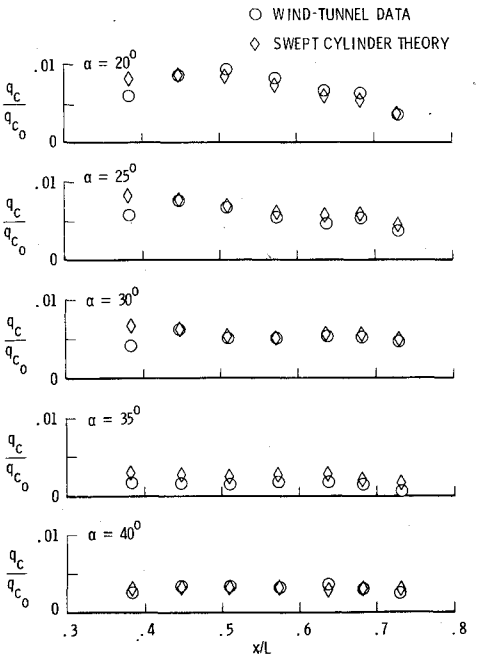

Fig. 13 Comparison of empirical swept cylinder theory with wind tunnel measurements for $M_\infty = 10$ and $Re_{\infty,L} = 2.4 \times 10^6$.

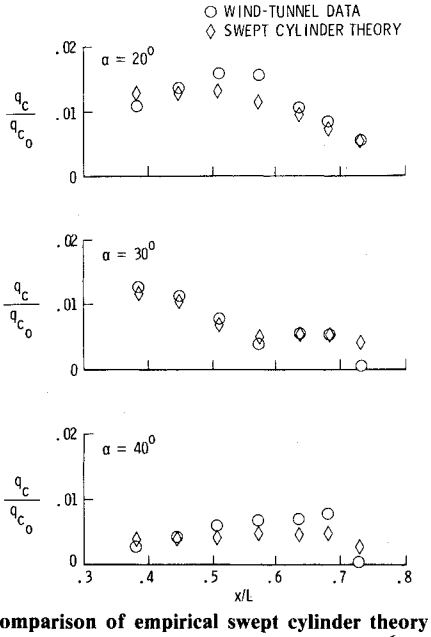

Fig. 14 Comparison of empirical swept cylinder theory with wind tunnel measurements for $M_\infty = 6$ and $Re_{\infty,L} = 2.7 \times 10^6$.

Comparison of Theory with Experiment

Although formulated using only a small portion of the wind-tunnel data, Eq. (7) was found to compare favorably with heating measurements obtained at all of the Mach 10 and Mach 6 test conditions. The close agreement between predicted and measured leeward centerline heating at Mach 10 is demonstrated in Figs. 11-13, which present comparisons with data for Reynolds numbers of 0.5×10^6, 1.0×10^6, and 2.4×10^6, respectively. The local heating rates are normalized, as described before, and the data for each Reynolds number are plotted as a function of axial location for each of the five angles of attack from 20-40 deg. Large variations in Mach 10 effective sweep angles shown in Fig. 5 translate into relatively large changes in top centerline heating. This is particularly evident in the low angle-of-attack and high Reynolds number data of Fig. 13. High angles of attack produced less change in

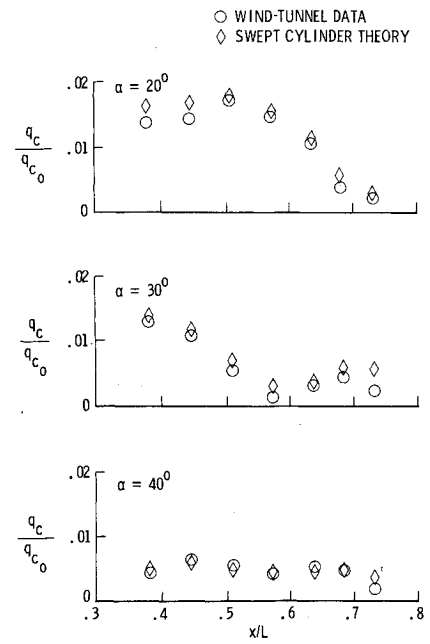

Fig. 15 Comparison of empirical swept cylinder theory with wind tunnel measurements for $M_\infty = 6$ and $Re_{\infty,L} = 5.4 \times 10^6$.

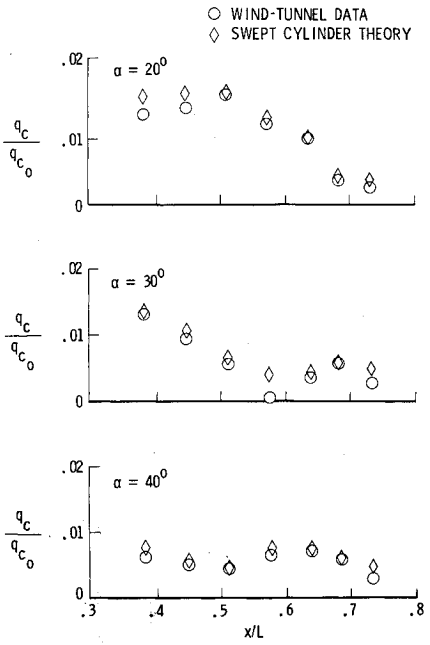

Fig. 16 Comparison of empirical swept cylinder theory with wind tunnel measurements for $M_\infty = 6$ and $Re_{\infty,L} = 7.3 \times 10^6$.

both sweep angle and heating distribution. Variations in the wind-tunnel data for higher angles of attack are at times somewhat larger than is predicted by the empirical method, but the difference between measurement and prediction is generally small and the theory preserves the overall trends of the data.

Figures 14-16 compare predictions of the swept cylinder theory with heat-transfer data obtained at $M_\infty = 6$ for Reynolds numbers 2.7×10^6, 5.4×10^6, and 7.3×10^6, respectively, at those angles of attack for which oil flow measurements are available. Again, the theory is in close general agreement with both the magnitude and trend of the wind-tunnel data, even though the character of the heating shown in these figures is different from that at Mach 10. The overall level of the Mach 6 data is higher and there is a greater variation in heating rates along the top centerline. The heating distributions occur in unique patterns that are strongly a function of angle of attack. This supports the original assessment, based on a comparison of effective sweep angles in Figs. 5 and 6, that test conditions at the lower Mach number produced a more dynamic leeside flowfield. Also, comparing the results at $\alpha = 20$ and 30 deg in Fig. 16 with the flow patterns shown in Figs. 7b and 7c serves to illustrate the ability of the empirical method to cope with a variety of surface flow conditions. Figures 11-16 show that the empirical swept cylinder theory applies over a wide range in Reynolds number and angle of attack, and over the Mach number range of 6-10. The theory's heating predictions are generally within 10-20% of measured values.

Conclusions

It has been shown that the Space Shuttle's leeward centerline can be thought of as being under the influence of a swept cylinder flowfield. The effective geometry of this flowfield, as well as the distribution of top centerline heating, can be directly related to oil flow patterns on the upper surface of the fuselage. Leeward centerline heating measurements were found to obey a modified form of a turbulent correlation that was originally designed for swept cylinder windward centerlines. The empirical swept cylinder heating method that has been developed accounts for the influence of the vortex-dominated leeside flowfield, but without having to compute detailed properties for that kind of flow. The heating method closely predicts experimental heat-transfer values on a 0.01-scale Shuttle model's leeward centerline corresponding to a variety of surface flow patterns at Mach numbers 6 and 10 over a wide range in Reynolds number and angle of attack.

Acknowledgments

The author wishes to thank J.C. Dunavant and P.F. Bradley for providing the experimental heating data used in this report.

References

[1]Schaefer, W.T. Jr., "Characteristics of Major Active Wind Tunnels at the Langley Research Center," NASA TM X-1130, 1965.

[2]Goldberg, T.J. and Hefner, J.N. (Appendix by Emery, J.C.), "Starting Phenomena for Hypersonic Inlets with Thick Turbulent Boundary Layers at Mach 6," NASA TN D-6280, 1971.

[3]Dunavant, J.C. and Stone, H.W., "Effects of Roughness on Heat Transfer to Hemisphere Cylinders at Mach Numbers 10.4 and 11.4," NASA TN D-3871, 1967.

[4]Fay, J.A. and Riddell, F.R., "Stagnation Point Heat Transfer in Dissociated Air," *Journal of Aeronautical Science*, Vol. 25, Feb. 1958, pp. 73-85.

[5]Zakkay, V., Miyazawa, M., and Wang, C.R., "Lee Surface Flow Phenomena Over Space Shuttle at Large Angles of Attack at $M_\infty = 6$," NASA CR-132501, 1974.

[6]Bertin, J.J., Senalug, G., McBride, M., and Willman, R.B., "The Effect of Surface Temperature and Reynolds Number on the Leeward Heat-Transfer for a Shuttle Orbiter," The University of Texas at Austin, Aerospace Engineering Rept. 75002, April 1975.

[7]Johnson, W.A., Memorandum A2-260-TH-59-218 made available by McDonnell Douglas Corp., Huntington Beach, Calif., unpublished work.

[8]Beckwith, I.E. and Gallagher, J.J., "Local Heat Transfer and Recovery Temperatures on a Yawed Cylinder at a Mach Number of 4.15 and High Reynolds Numbers," NASA Memorandum 2-27-59L, 1959.

[9]Beckwith, I.E. and Gallagher, J.J., "Experimental Investigation of the Effect of Boundary-Layer Transition on the Average Heat Transfer to a Yawed Cylinder in Supersonic Flow," NACA RM L56E09, 1956.

[10]O'Neal, R.L. and Bond, A.C., "Heat Transfer to 0° and 75° Swept Blunt Leading Edges in Free Flight at Mach Numbers from 1.90 to 3.07," NACA RM L58A13, 1958.

[11]Bond, A.C. and Feller, O.V., "Aerodynamic Heat Transfer to Wing Surfaces and Wing Leading Edge," NACA RM L57D22c, 1957.

[12]Hender, D.R., "A Miniature Version of the JA70 Aerodynamic Heating Computer Program, H800 (MINIVER)," McDonnell Douglas Astronautics Co. Rept. MDC G0462, June 1970, revised Jan. 1972.